

RADIATION-DRIVEN DYNAMIC TARGET RESPONSE FOR DISSIMILAR MATERIAL JETTING AND FOR DEBRIS EFFECTS IN PARTITIONED PIPES

R. J. Lawrence, M. D. Furnish, T. A. Haill, T. G. Trucano, T. A. Mehlhorn,
K. G. Budge, C. A. Hall, J. R. Asay, K. R. Cochrane,^a and J. J. MacFarlane^b

Sandia National Laboratories, Albuquerque, New Mexico 87185 USA*

^a*Ktech Corporation, Albuquerque, New Mexico 87106 USA*

^b*Prism Computational Sciences, Inc., Madison, Wisconsin 53703 USA*

ALEGRA is one of the principal computer codes being used at Sandia National Laboratories for simulating the dynamic material response of complex configurations. It solves shock physics problems in three spatial dimensions using Lagrangian, Eulerian, and/or ALE coordinates. The code runs on massively parallel computers, and contains a large variety of physics options including MHD, hydrodynamics, material strength and failure, radiation transport, conduction, and others. Two problems addressed recently consider the response of solid targets to short high-power and high-energy radiation loads.

The first problem involves a 100-micron-scale aluminum pin surrounded by a gold washer, which was exposed to a nominal 5-ns x-ray load from a NOVA laser-driven hohlraum at Lawrence Livermore National Laboratory. The differences in material properties lead to extensive jetting phenomena along the cylindrical axis of symmetry. This configuration has been scaled up physically by an order of magnitude for qualitatively similar experiments on the Sandia Z-pinch machine, where a nominal 50-ns-wide radiation pulse can be employed. Both configurations were simulated with the ALEGRA code. Subsequent calculations on the ALEGRA output using the imaging and spectral analysis code SPECT3D show that diagnostics using the Z-Beamlet Backlighter are feasible with this scaled up geometry.

The second problem examines the response of centimeter-scale cylindrical pipes that were exposed axially to high-energy radiation pulses generated by the Sandia Z-pinch machine. Two samples, one 5 cm long and one 10 cm long, were studied. The pipes contained partitions spaced along their length, the first of which was destroyed by the direct radiation load. The resulting cloud of debris penetrated and destroyed the subsequent partitions. Although there are discrepancies between the detailed experimental measurements and the numerical simulations, the calculations clearly illustrate the wide range of conditions involved in these experiments.

All of these calculations are leading to a better understanding of the diverse phenomena that these types of environments can generate. This important shock physics code illustrates numerical modeling techniques that are providing direct solutions to important applied problems in a predictive mode. Further, these studies are serving as ideal validation tools for this code, and in particular for its radiation transport option.

INTRODUCTION

The ALEGRA shock physics code (Boucheron *et al.*, 1999) is one of the principal computer codes being supported by the Accelerated Strategic Computing Initiative (ASCI) program. It solves shock physics problems in three spatial dimensions using Lagrangian, Eulerian, and/or ALE coordinates. The code runs on massively parallel computers, and contains a large variety of physics options including MHD, hydrodynamics, material strength and failure, radiation transport, conduction, and others. The code is being used widely to study, for example, the response of complex systems to high velocity impacts, the behavior of components under high explosive loading

* Sandia is a multiprogram laboratory operated by Sandia Corporation, a Lockheed Martin Company, for the United States Department of Energy under Contract DE-AC04-94AL85000.

conditions, and MHD-driven Z-pinch phenomena. Two problems that have been addressed recently consider the response of solid targets to short high-energy radiation loads.

The first problem involves a 100-micron-scale aluminum pin surrounded by a gold washer, which was exposed in a NOVA laser-driven hohlraum at Lawrence Livermore National Laboratory (LLNL) (Rosen *et al.*, 1998). The differences in material properties lead to extensive jetting phenomena along the cylindrical axis of symmetry. This configuration has been scaled up by an order of magnitude for qualitatively similar experiments on the Z-pinch machine at Sandia National Laboratories (SNL). Subsequent calculations employing the ALEGRA output and using the imaging and spectral analysis code SPECT3D (MacFarlane *et al.*, 2000) show that diagnostics using the Z-Beamlet Backlighter (ZBL) (Adams *et al.*, 1999) are feasible with this scaled up geometry.

The second problem examines the response of centimeter-scale cylindrical pipes, which were exposed to high-energy radiation pulses generated by the SNL Z-pinch machine (Furnish *et al.*, 2000). The pipes contained interior partitions or barriers spaced along their length, which were destroyed by the direct radiation load, and by the subsequent clouds of debris, respectively.

All of these calculations are leading to a better understanding of the diverse phenomena that these types of environments can generate. They are providing direct solutions to important applied problems in a predictive mode. Further, these studies will thus serve as ideal validation tools for this important shock physics code, and in particular for its radiation transport option.

RADIATION-DRIVEN JETS ON NOVA AND Z

To investigate the complex phenomena involved in jet formation when short high-power radiation pulses are incident on cylindrical configurations of dissimilar materials, we have used the ALEGRA code to study two different situations. The first configuration involves the simulation of actual experiments conducted on the NOVA laser facility at LLNL, for which Rosen *et al.* (1998) provide the details. The second is associated with a factor-of-ten scale-up of the configuration for exposure on the SNL Z-pinch facility. The configuration and geometry for the NOVA experiments

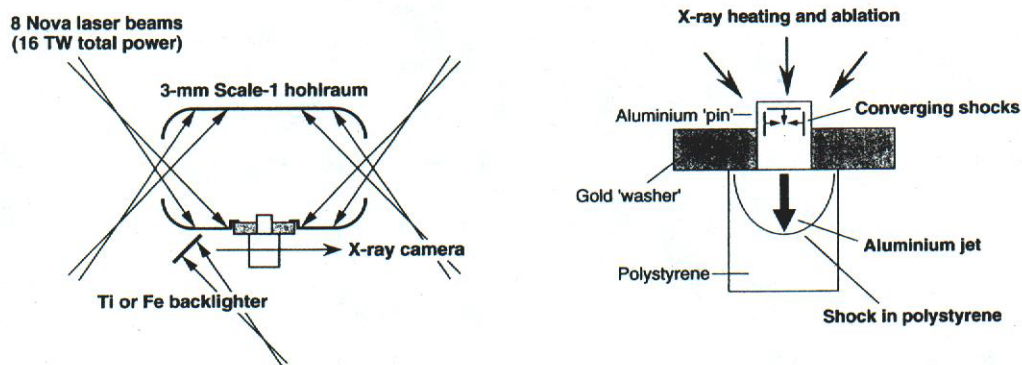


FIGURE 1. Geometry and configuration for NOVA experiments. Shown are the target in the hohlraum and the backlighter location (*left*), and the details of the target (*right*). The aluminum 'pin' has a diameter of 200 μm and is 150 μm long, the gold 'washer' is 50 μm thick, and the polystyrene backing has a diameter of 380 μm .

are shown in Fig. 1, and the radiation environment for these experiments is given in Fig. 2. For comparison, the latter figure also shows one of several possibilities for the radiative drive from the Z-pinch machine. Both represent Planckian time histories. The geometric scale-up was driven by

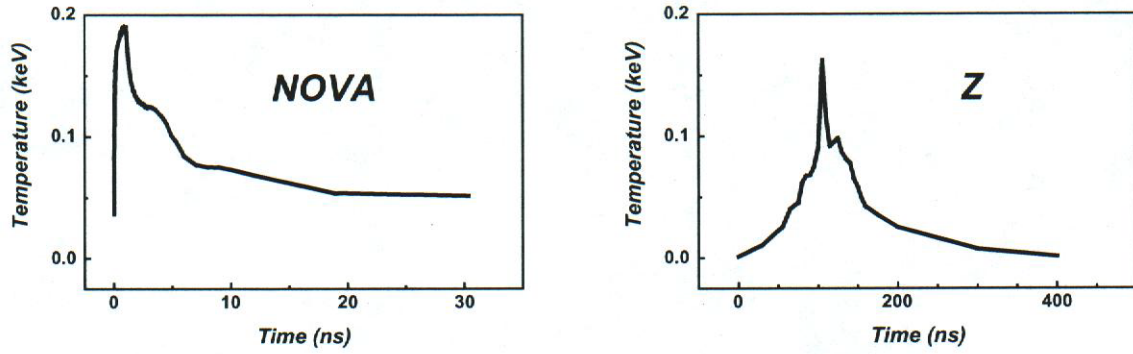


FIGURE 2. Assumed black-body temperature histories for the NOVA hohlraum (*left*), and the Z-pinch source (*right*). For NOVA the source has a peak temperature of ~ 190 eV and a FWHM pulse width of ~ 5 ns; the Z-pinch source has a peak of ~ 160 eV and a pulse width of ~ 50 ns. Note also that the rise-time for the Z pulse is substantially longer than that for NOVA—it could be reduced easily through the use of a thin burn-through foil, if desired.

the radiation pulse widths, which are 5 ns for NOVA and ~ 50 ns for Z. The estimated total energy fluences on the samples are high—about 0.25 MJ/cm^2 for the NOVA source, and almost 0.7 MJ/cm^2 for the Z-pinch. The peak powers for the two cases are $\sim 130 \text{ TW/cm}^2$ and $\sim 70 \text{ TW/cm}^2$ respectively. Thus Z gives an energy fluence higher by a factor of about three, but NOVA yields a peak power greater by nearly a factor of two.

NOVA calculations and experimental comparisons. The ALEGRA calculations simulating the NOVA experiments employed a two-dimensional Eulerian mesh, with either $10\text{-}\mu\text{m}$ or $5\text{-}\mu\text{m}$ resolution. The former mesh had 4,500 elements and the latter had 18,000. The radiation flow was treated with a single-group SN_1 model. Both the coarse-zoned and fine-zoned calculations gave similar results, with the latter showing more detail in the jetting regions, as anticipated. The fine-zoned problem showed slightly faster ($\sim 9\%$) on-axis jet motion, so it is possible that the solution is not quite converged. Selected results of the calculations are shown in Fig. 3. Included in the figure are numerical simulations of the radiographs taken with the backlighter indicated in Fig. 1. In Table 1 we compare the present results with actual experimental radiographs (similar to those in Fig. 3, but with less detail), and with code calculations from Atomic Weapons Establishment (*PETRA*), LLNL (*CALE*), and Los Alamos National Laboratory (*RAGE*) (Rosen *et al.*, 1998). We have listed the axial positions of the leading edge of the jet as a function of time. These values show a fairly wide variation, but the ALEGRA results are consistent with the other analyses. The 9-ns experimental position seems to lag all the numerical results, but this may be due to lack of resolution. Even though the agreement is not ideal, we feel that ALEGRA is modeling the relevant phenomena in a realistic manner, and is consistent with other numerical approaches.

TABLE 1. Axial jet displacement (in μm) for various codes and the experiment. Although there is a wide variation, the ALEGRA calculations are consistent with the other results.

Code	ALEGRA (Eulerian)	PETRA (Eulerian)	CALE (ALE)	RAGE (AMR)	Experiment (Estimated)
Time = 6 ns	265	245	300	280	~ 260
Time = 9 ns	380	345	405	380	300+

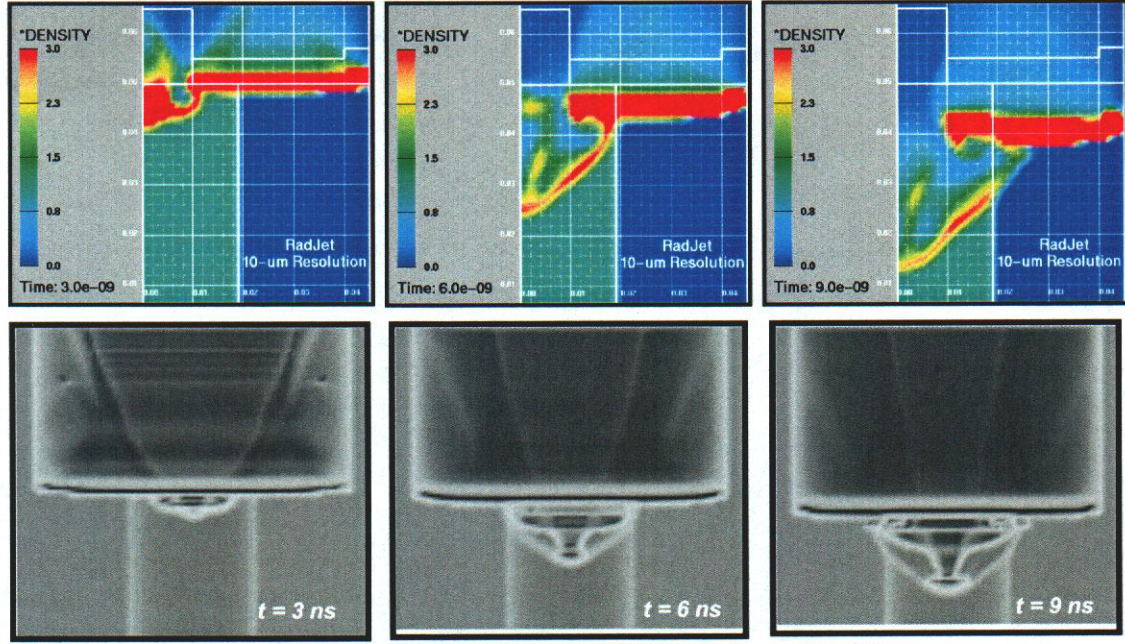


FIGURE 3. Selected output from the NOVA-driven jet calculation. The upper row shows density plots from the ALEGRA output at times of 3, 6, and 9 ns. The lower row gives simulated backlighter radiographs for the same times, as generated by the SPECT3D code.

Configuration scale-up and Z-pinch calculations. In considering how similar experiments would be conducted on the SNL Z machine, we first noted that radiation pulse widths about an order of magnitude longer were available. This immediately suggested that we should be able to

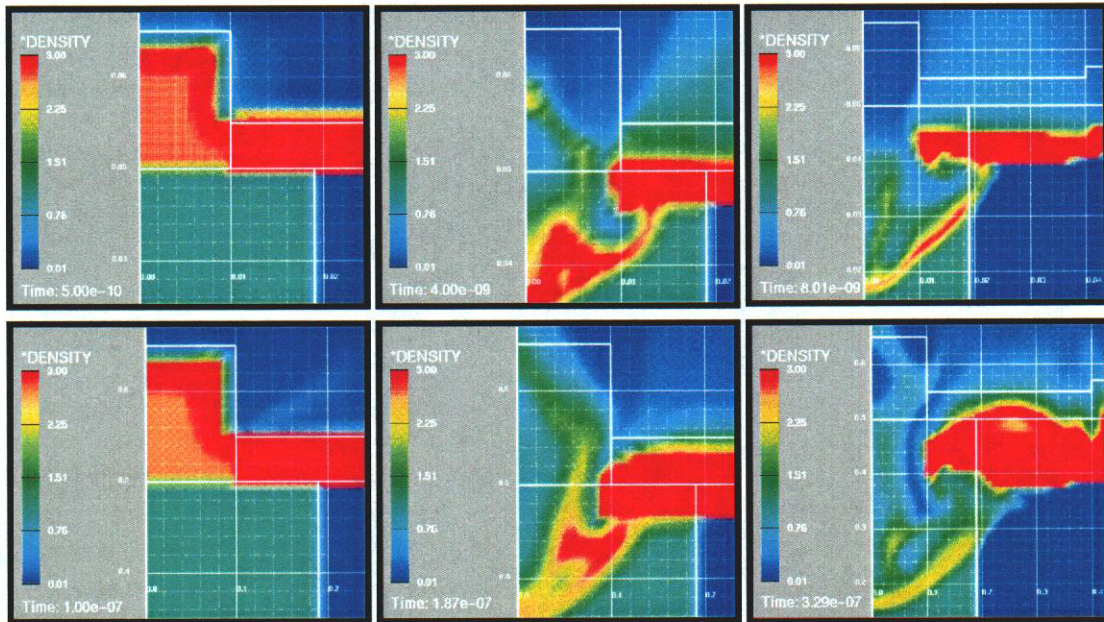


FIGURE 4. Comparisons between NOVA and Z calculations. The upper row is for the NOVA configuration, and the lower row is for the factor-of-ten scale-up for Z. Times were chosen for similar stages in the evolution of the response. Density is in g/cm^3 , time is in s, and dimensions are in cm.

scale-up the physical dimensions of the configuration by a comparable factor. Although the phenomena associated with radiation transport will not scale in the simple manner that should apply to purely mechanical and time variables, the overall response should be qualitatively similar. Other, but smaller departures from homologous behavior result from the differences in the shapes of the radiation histories shown in Fig. 2, in particular the slower rise time for the Z source. Nonetheless, when we plot computational results for comparable stages in the evolution of the response, the material densities look quite similar, as shown in Fig. 4. It should be mentioned that the temperatures and pressures show greater differences, especially in terms of their maximum values. For example at 4 ns for the NOVA problem and $0.2\ \mu\text{s}$ for Z, the peak temperatures are 130 eV and 50 eV, respectively. Similarly, the peak pressures are 30 Mb and 3 Mb. Later, at 12 ns for NOVA and $0.4\ \mu\text{s}$ for Z, the peak values have decayed, to 70 eV and 20 eV for the temperatures, and 4 Mb and 0.5 Mb for the pressures. Because of the shorter pulse width and higher power, the NOVA configuration thus gives temperatures greater by nearly a factor of three and pressures higher by roughly a factor of ten, when compared with the Z results.

With the larger physical size for the Z setup, there is some concern that the main diagnostic tool for observing the experiment, the Z-Beamlet Backlighter (Adams, *et al.*, 1999), may not be able to penetrate the jet. To examine this aspect of the problem, we have used the imaging and spectral analysis code SPECT3D (MacFarlane *et al.*, 2000) to post-process the output from the ALEGRA calculations. Note that backlighter performance depends not only on photon energy but on conversion efficiency and many other issues; we are only looking at the former here. Depending on the backlighter target material, photon energies from 3 to 10 keV should be available. For example, using the lower energies, at reasonable times and through the main body of the jet, the code yields optical depths that are ~ 20 at 3 keV, ~ 10 at 6 keV, and 5 to 6 at 8 keV. These optical thicknesses would make this type of measurement very difficult, at best. However, with a backlighter photon energy of 10 keV, which should be possible, the optical depth would

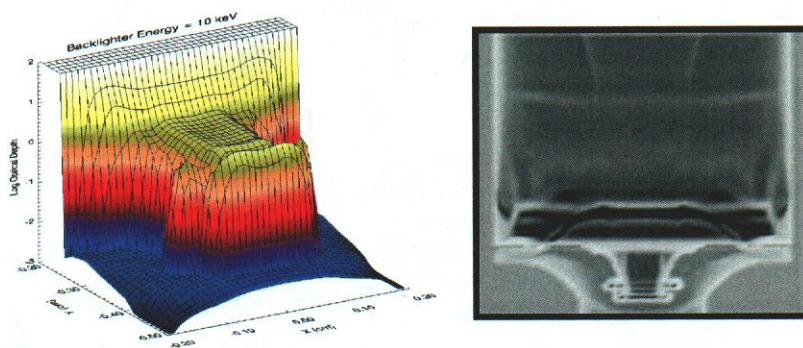


Figure 5. Visualization (*left*) and simulated radiograph (*right*) of jet at 528 ns for the Z calculation. The backlighter photon energy was chosen as 10 keV. On the visualization, the amplitude of each cell represents the optical depth through the jet as a function of axial position (Y) and offset from the axis (X).

be of order unity, or maybe just a little greater, which is an acceptable value. It is this last case that is illustrated in Fig. 5, where we show the optical depth both in a 3-D visualization of the jet and in a simulated radiograph. We thus conclude that with a 10 keV backlighter these experimental measurements should be possible.

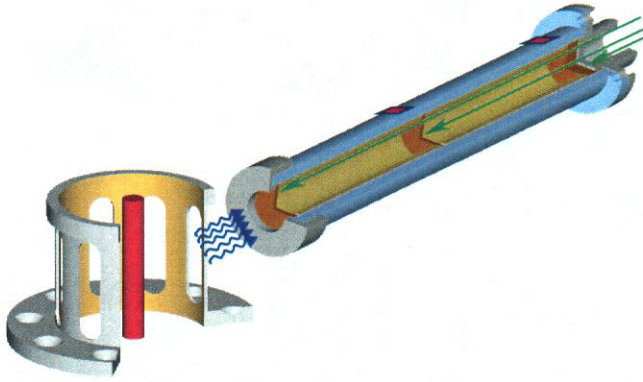


FIGURE 6. Schematic of debris propagation experiments on Z. The Z-pinch is shown in the center of the slotted-can hohlraum. Its x ray energy is incident on the front partition of the pipe. The arrows inside the pipe represent 12 velocity interferometers for measuring the velocity histories of the three partitions across the pipe. Two experiments were conducted, one with a 10-cm-long pipe, and the other with a 5-cm-long pipe—the partitions were spaced uniformly in both cases.

RADIATION LOADS ON A PARTITIONED PIPE

In experiments such as those described above, in particular on the Z machine, there is always the risk of experiment failure due to impact by x-ray-driven debris. To study these phenomena we recently conducted two experiments involving heavily instrumented tubular structures (Furnish *et al.*, 2000). One of the pipes was 10 cm long, and the other was 5 cm in length. They were exposed end-on to the radiation from a slotted-can hohlraum, which was in turn driven by a collapsing Z-pinch wire array. The measured Planckian time history from this source was shown earlier, in Fig. 2—in fact, these experiments were the origin for the radiation drive used in the Z-pinch jet calculations described in the previous section. A schematic of the experimental arrangement is shown in Fig. 6, in which we can see the pipe with its three partitions, the pinch and the slotted-can hohlraum, and indications for the diagnostic instrumentation. Taking into account the geometry of the setup, we estimate that the total energy fluence incident on the front partition was $\sim 23 \text{ kJ/cm}^2$ for both the long- and short-pipe experiments. As shown, both experiments contained multiple velocity interferometer diagnostics to measure the velocity histories of each of the three partitions. In addition, strain gages were mounted on the outside walls of the pipes, but they did not function properly because of electrical noise.

Pre-shot calculations. To aid in the experimental design, we performed several calculations using a simplified radiation input. Specifically, we looked at the 10-cm-long pipe with 40-ns-wide

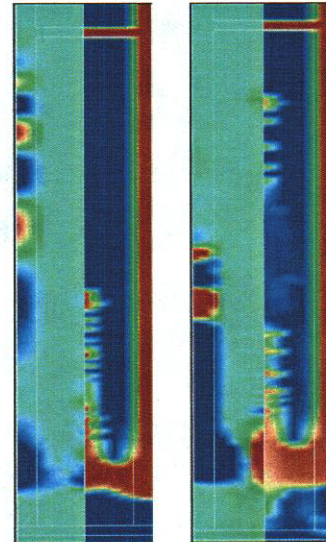


FIGURE 7. Representative images from the pre-shot calculations. The first (*left*) is for the low-fluence case ($T_{\text{max}} = 55 \text{ eV}$, $\Phi \approx 19 \text{ kJ/cm}^2$), and the other (*right*) is for the high-fluence calculation ($T_{\text{max}} = 100 \text{ eV}$, $\Phi \approx 200 \text{ kJ/cm}^2$). In each of the two plots the left side indicates pressure and the right side shows density. Both cases are for the long-pipe, and only the region between the front and middle partitions is shown.

triangular pulses peaking at both 55 and 100 eV, with no geometric attenuation. The resulting fluences were ~ 19 and ~ 200 kJ/cm², respectively, thus differing by almost a factor of 11. These results revealed two distinct regimes for the target response, which are illustrated in Fig. 7. For the lower fluence case the stress waves moving up the pipe walls precede the debris by almost a factor of two in time. At the higher fluence the reverse is true, *i.e.*, the debris precedes the wall signals by roughly the same factor of two. In both cases the debris contains sufficient energy and momentum to destroy the subsequent partitions. Based on these predictions the experiments were carried out at conditions approximating the low-fluence input.

Experimental results and numerical comparisons. The active velocity measurements functioned well, and usable data were obtained for all three partitions on both experiments. For both long and short pipes the front partitions were abruptly accelerated to ~ 2 km/s (2.2 km/s for the long tube, and 1.75 km/s for the short). The velocities for the middle barriers were measured as ~ 0.5 km/s for the long pipe and ~ 1 km/s for the short one. Similarly the rear partitions had velocities of ~ 120 m/s and ~ 100 m/s, respectively. For the latter two barriers, these are the motions that were induced by the debris clouds originating from the direct radiation loads on the front partitions and subsequently moving up the pipes. In addition, the VISAR records for the middle and rear partitions show smaller precursor motions from the stress waves moving up the walls of the pipes ahead of the debris. Also, both on-axis and off-axis measurements indicate that the debris is strongly peaked toward the center of the configuration. Finally, it should be noted that these data show significant scatter, indicating the variable nature of the phenomena we are trying to capture with these measurements.

Post-shot calculations using the best estimates for the radiation input show qualitatively similar results, but the magnitudes of the calculated debris velocities are roughly a factor of two greater than the above measurements. Important features that *are* matched include the peaking of the debris on

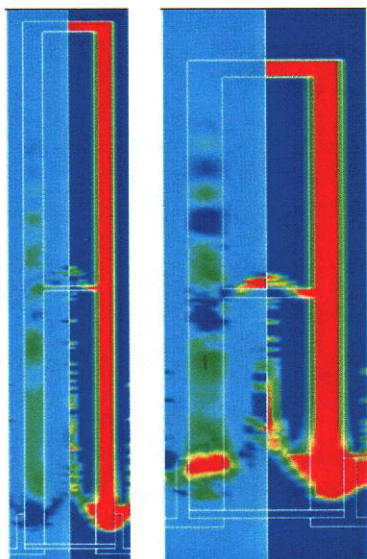


FIGURE 8. Post-shot calculations for the long pipe (*left*) and the short pipe (*right*). In both plots pressure is shown on the left side and density is on the right side. They are both for times just after the debris penetrates the middle partition— $t = 15$ μ s for the long pipe and $t = 8$ μ s for the short pipe. The fluence for both simulations was $\Phi \approx 23$ kJ/cm².

the cylindrical axis, and the fact that for these fluence levels the stress wave response of the pipe walls precedes the debris motion in the pipe interior. These features are indicated in the selected plots from the calculations shown in Fig. 8. The discrepancies in the magnitudes of the calculated velocities are not understood—a possibility could be that the experimental energy fluences incident

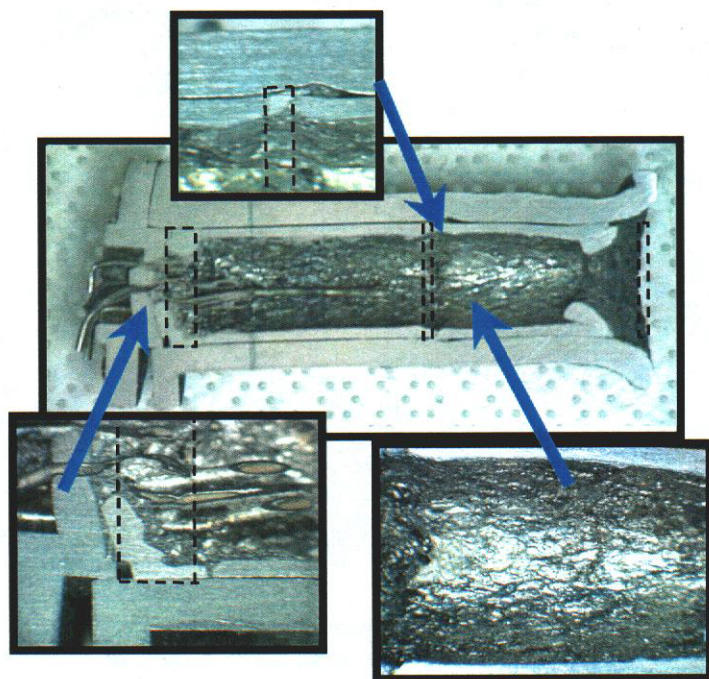


FIGURE 9. Post-test photographs of sectioned half of short pipe. The original locations of the partitions are indicated by the dashed rectangles. The x rays were incident from the right on the full-scale photo. The lower-left expanded view shows the remains of the thin hollow tubes that contained the optical probes for the velocity interferometers.

on the pipe ends were lower than estimated, however, we have no reason to either accept or reject this hypothesis.

Both pipes were recovered after the experiments, and the short tube was sectioned for both visual and metallographic analysis. Details of this examination have been provided by Furnish *et al.* (2000), but the observations clearly show that a combination of violent processes occurred. In particular, the metal debris lining the inside of the pipe cooled from a melted state; the front and middle partitions were completely melted, and at least the front of the front partition was vaporized. Several of the photos from this analysis are shown in Fig. 9. These results are consistent with both the velocity measurements and the calculations.

CONCLUSIONS

For the radiation-driven jet problem we have provided validation for the ALEGRA models through comparison with the NOVA experiment and other calculations. We have shown that experiments scaled up by an order of magnitude in size on Z yield qualitatively similar dynamic response phenomenology. Based on the calculations, and with the aid of additional visualization and analysis software, we have also shown that diagnostics using the ZBL for the scaled-up experiments are feasible.

For the partitioned pipe experiments we used ALEGRA in a predictive mode to help with experimental design, and in this process the analysis revealed qualitatively different response phenomenology under variations in loading conditions. Although detailed comparisons with measured velocity histories were not as successful as hoped, the numerical modeling qualitatively simulated all the major phenomenology observed in the experiments. With this problem, new applied capabilities for both Z and ALEGRA have been demonstrated.

Finally, we emphasize that the ASCI code ALEGRA is under continuing development, but as shown here, it is also being used routinely to address practical issues associated with experimental design and with applied component-level response of real interest.

REFERENCES

Boucheron, E. A., *et al.*, *ALEGRA: User Input and Physics Descriptions—OCT 99 Release*, SAND99-3012, Sandia National Laboratories, Albuquerque, New Mexico, 1999.

Rosen, P. A., M. Fell, J. M. Foster, T. S. Perry, P. E. Stry, B. H. Wilde, “Radiation-Driven Supersonic-Jet Experiments,” presentation at the 40th Annual Meeting, American Physical Society, Division of Plasma Physics, New Orleans, Louisiana, 1998.

Adams, Richard, *et al.*, *Advanced Conceptual Design Report For the Z-Beamlet Laser Backlighter System*, UCRL-ID-134409, Lawrence Livermore National Laboratory, Livermore, California / Sandia National Laboratories, Albuquerque, New Mexico, 1999.

MacFarlane, J. J., A. R. Thomas-Cramer, P. Zeng, K. A. Park, *SPECT3D—Imaging and Spectral Analysis Suite*, PCS-R-015, PRISM Computational Sciences, Inc., Madison, Wisconsin, 2000.

Furnish, M. D., R. J. Lawrence, C. A. Hall, J. R. Asay, D. R. Barker, G. A. Mize, E. A. Marsh, M. A. Bernard, “Radiation-Driven Shock and Debris Propagation Down a Partitioned Pipe,” *International Journal of Impact Engineering* [to be published], 2000.